Coordination Chemistry Reviews 255 (2011) 2058–2067

Contents lists available at ScienceDirect

Coordination Chemistry Reviews

journal homepage: www.elsevier.com/locate/ccr

Review

Supramolecular aspects of iron(II) crown-dipyridyl spin-crossover compounds

Ian A. Gass, Stuart R. Batten, Craig M. Forsyth, Boujemaa Moubaraki, Caspar J. Schneider, Keith S. Murray*

School of Chemistry, Monash University, Building 23, Clayton, Victoria 3800, Australia

Contents

ARTICLE INFO

Article history:
Received 29 November 2010
Accepted 20 January 2011
Available online 27 January 2011

Keywords:
Supramolecular
Iron(II)
Spin-crossover
Magnetism
Structure
Crown-ether
Host–guest

ABSTRACT

The synthesis, structures and magnetism of the complexes $[Fe^{II}(3\text{-bpp})_2][bpmdcK](SeCN)_{1.7}(ClO_4)_{1.3}\cdot MeOH\cdot H_2O$ (**1**), $[Fe^{II}(3\text{-bpp})_2]_4[bpmdcH_2(H_2O)_2](ClO_4)_{10}\cdot 7H_2O\cdot 3MeOH$ (**2**) and *cis*-$[Fe^{II}_2(NCSe)_2((3,5\text{-}Me_2pz)_3CH)_2(\mu\text{-bpmdc})]\cdot 2MeCN$ (**3**) (where 3-bpp = 2,6-di(pyrazole-3yl)pyridine, bpmdc = *N*,*N*′-bis(4-pyridyl-methyl)diaza-18-crown-6) and $(3,5\text{-}Me_2pz)_3CH$ = tris(3,5-dimethylpyrazole)methane, are presented. These compounds form a study of the supramolecular influence of host–guest/crown-ether interactions and cation-to-crown hydrogen-bonding effects upon d^6 spin transitions, the latter occurring above, or near to, room temperature in **1** and **2**. Desolvation effects also influence the $T_{1/2}$ values. The dinuclear compound **3** contains covalent pyridyl (crown) N to Fe bridge bonding and remains high spin.
© 2011 Elsevier B.V. All rights reserved.

1. Introduction

The spin crossover (SCO) phenomenon originates from the ligand environment around d^n (n = 4–7) first row transition metals which enforce an energetically delicate balance between the low and high spin states of the ion in question. This delicate balance can be perturbed by temperature, light and pressure leading to molecules that can exist in two different electronic states [1]. Fe(II) complexes with a typical octahedral $[FeN_6]^{2+}$ environment are among the most studied examples of SCO systems where the two spin states of the iron are the singlet $^1A_1$ (diamagnetic, low-spin(LS)) and the quintet $^5T_2$ (paramagnetic, high-spin(HS)). SCO properties are derived not only from a ligand system with an appropriate ligand field strength, but also from cooperativity between the complexes in the solid state leading to a variety of interesting SCO features such as one and two step, gradual and abrupt, complete and incomplete transitions and thermal hysteresis [2]. Strong cooperativity between the spin centres can induce thermal hysteresis loops with widths up to 60 K [3] with their history dependent bistability leading to the possibility of uses in applications such as sensors, molecular switches, displays and data storage [4].

* Corresponding author. Tel.: +61 399054512; fax: +61 399054597.
E-mail address: keith.murray@monash.edu (K.S. Murray).

0010-8545/$ – see front matter © 2011 Elsevier B.V. All rights reserved.
doi:10.1016/j.ccr.2011.01.033

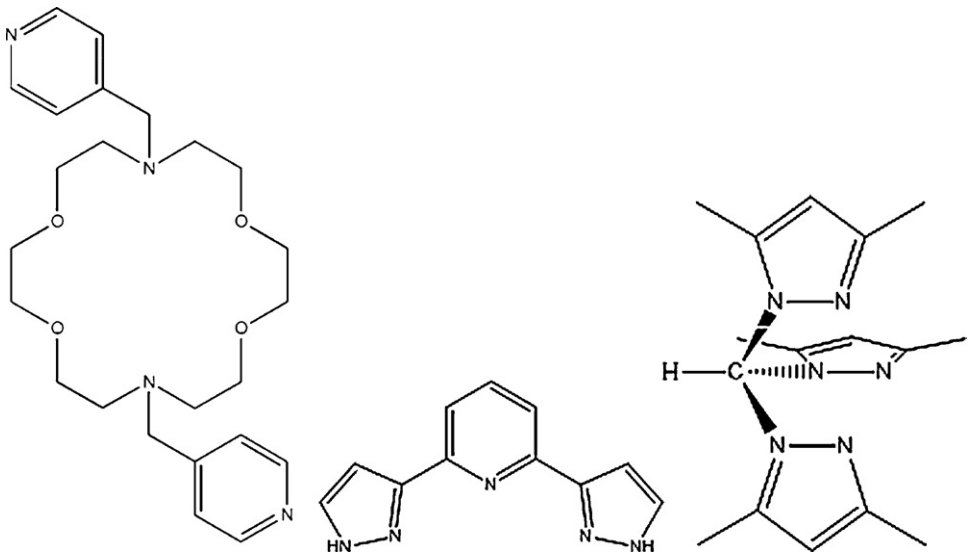

Scheme 1. Structural formulae of the ligands bpmdc (left), 3-bpp (centre) and (3,5-Me_2pz)$_3$CH (right). *N.B.* The other isomer, 2,6-di(pyrazole-1-yl)pyridine also forms numerous SCO Fe(II) compounds and it is often labelled 1-bpp [11]. It is also labelled 2,6-di(pyrazole-3-yl)pyridine [12].

Strong cooperativity in SCO systems is thought to stem from covalent linkers [5], NH/π and CH/π interactions [6], van der Waals short contacts [7], hydrogen bonds [8] and π–π stacking [9]. To achieve a large thermal hysteresis centred around ambient temperature [10] such interactions must be taken into account when choosing a ligand system. A moderate ligand field strength around the metal ion may simply not be enough and the addition of some non-coordinating substituent's may encourage strong cooperativity via the aforementioned interactions. Coordinating pyridine nitrogen atoms and imine-type pyrazolyl nitrogens on 2,6-di(pyrazole-3-yl)pyridine (3-bpp; see caption to Scheme 1 concerning labelling and the other ligand isomer 1-bpp [11,12]) encapsulate an $[FeN_6]^{2+}$ distorted octahedral environment, while the non-coordinating NH groups on the pyrazolyl rings encourage hydrogen bonding to anions and solvent. The subsequent increase in acidity of the N-H group will increase the electron density on the coordinating imine nitrogen atom which strengthens the imine nitrogen–iron σ bond which has obvious ramifications for any observed SCO properties [13]. It has also been suggested that cooperativity in the dehydrated forms of salts such as $[Fe(3\text{-bpp})_2]X_2{\cdot}H_2O$ is enhanced by the formation of a two-dimensional net of terpy like embraces which allow edge-to-face (ef) and offset face-to-face (off) interactions [14].

The majority of the characterised Fe(II) salts of 3-bpp are of the $[Fe(3\text{-bpp})_2]X_2{\cdot}H_2O$ type (see Table 1) with other solvates including methanol, [26–30] methanol/water [27] and acetonitrile [29]. A recent review of the $[Fe(3\text{-bpp})_2]X_2{\cdot}H_2O$ salts [12] reveals that at ambient temperatures the fully hydrated species are generally in the diamagnetic singlet $^1A_1$ state, whereas the anhydrous species are in the paramagnetic quintet $^5T_2$ state. As the series progresses from the hydrated form to the anhydrous form the $T_{1/2}$ values decrease while the high to low spin transition character changes from gradual to abrupt with associated thermal hysteresis. For example $[Fe(3\text{-bpp})_2][BF_4]_2{\cdot}3H_2O$ has a $T_{1/2}$ value of 288 K with a gradual transition, whereas in $[Fe(3\text{-bpp})_2][BF_4]_2$ the $T_{1/2}$ value is 176 K and this abrupt transition has a 10 K thermal hysteresis [13a,13b,15,16,24]. The nature of the spin transition and the magnitude of the $T_{1/2}$ value is therefore dependent on the degree of solvation, and on the presence or absence of any significant interactions between the spin centres such as a hydrogen bonded network and/or any aryl–aryl interactions. Other d- and f-block 3-bpp metal salts are known [31,32] and have also been reviewed [12].

(*N,N′*-bis(4-pyridyl-methyl)diaza-18-crown-6) (bpmdc) is a flexible pyridyl based ligand which incorporates a diaza 18-crown-6 whose length and overall geometry depends on the presence of guests, such as s-block ions, held within the crown ring [17]. Our initial aim in this work was actually to make dinuclear Fe(II) SCO complexes bridged by bpmdc in the way reported recently by Rosa and co-workers for a 4,4′-bipyridine (bipy) analogue, $[\{Fe^{II}(3\text{-bpp})(NCS)_2\}_2(\mu\text{-}4,4'\text{-bipy})]$ [29]. In particular, we were interested to see if changing a guest cation in the bpmdc ring would influence the SCO behaviour at the Fe(II) centres, the latter being bonded some distance away via the pyridyl N atoms. There have been only a few such studies reported on guest interactions and these were with monomeric Fe(III) SCO compounds containing crown-attached Schiff base ligands [22a]. In a similar vein a series of Fe(III) Schiff base complexes were shown to display cation dependent spin states [22b] but to our knowledge, none have involved di- or polynuclear Fe species. In a separate study, we have used other crown-attached N,N-chelators of the dipyridylamine type to make polynuclear Fe(II) materials [33].

Despite many attempts to control the 3-bpp to Fe(II) ratio to 1:1, and obtain covalent bridging by bpmdc, the 1:2 Fe(3-bpp)$_2$ stoichiometry was invariably isolated. Hence, reactions of $Fe(II)(ClO_4)_2{\cdot}6H_2O$ with KNCSe, bpmdc and 3-bpp yielded not the expected dimer but the rather unusual, and structurally attractive, hydrogen-bonded (pyrazole) network compound $[Fe^{II}(3\text{-bpp})_2][bpmdcK](ClO_4)(NCSe)_2$ (**1**). Leaving out KNCSe from the reaction led to H_2O being in the crown and isolation of $[Fe^{II}(3\text{-bpp})_2]_4[bpmdcH_2(H_2O)_2](ClO_4)_{10}$ (**2**). We were, however, able to prepare a bpmdc-bridged dinuclear complex, *cis*-$[Fe_2(NCSe)_4((3,5\text{-}Me_2pz)_3CH)_2(\mu\text{-bpmdc})]$ (**3**), a bpmdc analogue of *cis*-$[Fe_2(NCSe)_4(3,5\text{-}Me_2pz)_3CH)_2(\mu\text{-}4,4'\text{-bipy})]$ [36c], that has *fac*-tridentate tris(3,5-dimethylpyrazole)methane end groups, rather than 3-bpp, and with two $NCSe^-$ ligands making up the octahedron around each Fe^{II}. Tris-pyrazolylmethane ligands are known to induce SCO in mononuclear [34,35] and dinuclear [36] Fe^{II} compounds, usually when two such ligands make up the FeN_6 ligand-field.

Table 1
Summary of known Fe(II) salts of 3-bpp and the present 'crown' derivatives, **1** and **2**.

Formula	Reference	Formula	Reference
$[Fe(3\text{-bpp})_2][ClO_4]_2$	[13a]	$[Fe(3\text{-bpp})_2][Cr(bpy)(ox)_2]_2{\cdot}2H_2O$	[27,28]
$[Fe(3\text{-bpp})_2][ClO_4]_2{\cdot}H_2O$	[13a]	$[Fe(3\text{-bpp})_2][Cr(bpy)(ox)_2]_2$	[27,28]
$[Fe(3\text{-bpp})_2][ClO_4]_2{\cdot}3H_2O$	[13a]	$[Fe(3\text{-bpp})_2][Cr(bpy)(ox)_2]_2{\cdot}2H_2O(r)$	[27,28]
$[Fe(3\text{-bpp})_2][BF_4]_2$	[15,13a,16,24]	$[Fe(3\text{-bpp})_2][Cr(bpy)(ox)_2]_2{\cdot}MeOH$	[27,28]
$[Fe(3\text{-bpp})_2][BF_4]_2{\cdot}2H_2O$	[13a]	$[Fe(3\text{-bpp})_2][Cr(phen)(ox)_2]_2{\cdot}0{\cdot}5H_2O{\cdot}0.5MeOH$	[27]
$[Fe(3\text{-bpp})_2][BF_4]_2{\cdot}3H_2O$	[13b,24]	$[Fe(3\text{-bpp})_2][Cr(phen)(ox)_2]_2$	[27]
$[Fe(3\text{-bpp})_2][PF_6]_2$	[13b,24]	$[Fe(3\text{-bpp})_2][Cr(phen)(ox)_2]_2{\cdot}0{\cdot}5H_2O$	[27]
$[Fe(3\text{-bpp})_2][PF_6]_2{\cdot}H_2O$	[13b]	$[Fe(3\text{-bpp})_2][Cr(phen)(ox)_2]_2{\cdot}5{\cdot}5H_2O{\cdot}2.5MeOH$	[27]
$[Fe(3\text{-bpp})_2][PF_6]_2{\cdot}2H_2O$	[13b]	$[\{Fe(3\text{-bpp})(NCS)_2\}_2(4,4'\text{-bipy})]{\cdot}2MeOH$	[29]
$[Fe(3\text{-bpp})_2][PF_6]_2{\cdot}3H_2O$	[24]	$[Fe(3\text{-bpp})_2][Cu(pds)_2]_2{\cdot}3CH_3CN$	[30]
$[Fe(3\text{-bpp})_2][NO_3]_2{\cdot}2H_2O$	[13b]	$[Fe(3\text{-bpp})_2][Cu(pds)_2]_2{\cdot}2.5CH_3OH$	[30]
$[Fe(3\text{-bpp})_2]Br_2$	[13b,24]	$[Fe^{II}(3\text{-bpp})_2][bpmdcK](SeCN)_{1.7}(ClO_4)_{1.3}{\cdot}MeOH{\cdot}H_2O$ **1**	tw
$[Fe(3\text{-bpp})_2]Br_2{\cdot}5H_2O$	[13b,24]	$[Fe^{II}(3\text{-bpp})_2]_4[bpmdcH_2(H_2O)_2](ClO_4)_{10}{\cdot}7H_2O{\cdot}3MeOH$ **2**	tw
$[Fe(3\text{-bpp})_2]I_2$	[13b,24]		
$[Fe(3\text{-bpp})_2]I_2{\cdot}2H_2O$	[24]		
$[Fe(3\text{-bpp})_2]I_2{\cdot}4H_2O$	[13b]		
$[Fe(3\text{-bpp})_2][CF_3SO_3]_2$	[18]		
$[Fe(3\text{-bpp})_2][CF_3SO_3]_2{\cdot}H_2O$	[18,19]		
$[Fe(3\text{-bpp})_2][CF_3SO_3]_2{\cdot}3H_2O$	[18]		
$[Fe(3\text{-bpp})_2][NCS]_2{\cdot}2H_2O$	[20,21,24]		
$[Fe(3\text{-bpp})_2][NCSe]_2$	[20,21,24]		
$[Fe(3\text{-bpp})_2][Fe(CN)_5(NO)]$	[14]		
$[Fe(3\text{-bpp})_2]_2[Cr(C_2O_4)_3]ClO_4{\cdot}5H_2O$	[23]		
$[Fe(3\text{-bpp})_2]Cl_2{\cdot}6.5H_2O$	[25]		
$[Fe(3\text{-bpp})_2][MnCr(ox)_3]_2{\cdot}bpp{\cdot}CH_3OH$	[26]		

Abbreviations. ox, oxalate; bpy, 2,2′-bipyridine; phen, 1,10-phenanthroline; 4,4′-bipy, 4,4′-bipyridine; pds, pyrazine-2,3-diselenolate; tw, this work.

2. Experimental

2.1. Syntheses

All manipulations were carried out under aerobic conditions using chemicals as received, unless otherwise stated. *Caution*! Care should be taken when using the potentially explosive perchlorate anion. The ligands *N,N′*-bis(4-pyridyl-methyl)diaza-18-crown-6) (bpmdc) and 2,6 di(pyrazole-3yl) pyridine (3-bpp) were prepared by use of reported methods [37,38], as was the precursor iron(II) complex $[Fe^{II}((3,5\text{-}Me_2pz)_3CH)(OH_2)_3][BF_4]_2$ [39].

$[Fe^{II}(3\text{-bpp})_2][bpmdcK](SeCN)_{1.7}(ClO_4)_{1.3}{\cdot}MeOH{\cdot}H_2O$ (1). $Fe(ClO_4)_2{\cdot}6H_2O$ (57.3 mg, 0.158 mmol) in 5 ml methanol was treated with 3-bpp (33.7 mg, 0.158 mmol), KSeCN (45.6 mg, 0.316 mmol) and L-ascorbic acid (15 mg, 0.087 mmol) and stirred for 5 min. This was then added to 1 ml of an ethanolic solution of bpmdc (35.2 mg, 0.0791 mmol) in 5 ml dichloromethane and stirred for a further 2 min then filtered. The solution was then layered with diethyl ether to produce X-ray quality crystals in 2 weeks in 63% yield (65 mg). The sample analysed as **1**·$MeOH{\cdot}H_2O$ *viz.* $FeC_{48.7}H_{60}N_{15.7}O_{11.2}Se_{1.7}K_1Cl_{1.3}$. Found (calc.%): C 44.31 (44.32), H 4.65 (4.58), N 15.54 (16.66). In the course of the SQUID measurement the sample was heated to 400 K and this then analysed as anhydrous **1**. Found (calc.%): C 45.11 (45.12), H 4.18 (4.29), N 17.16 (17.32).

$[Fe^{II}(3\text{-bpp})_2]_4[bpmdcH_2(H_2O)_2](ClO_4)_{10}{\cdot}7H_2O$ 3MeOH (2). 2 ml of an ethanolic solution of bpmdc (42.8 mg, 0.0963 mmol) and $KClO_4$ (13.4 mg, 0.0963 mmol) dissolved in 5 ml of a methanol/dichloromethane (1:1, v:v) solution and stirred for 30 min. This was then added to a solution of $Fe(ClO_4)_2{\cdot}6H_2O$ (70 mg, 0.192 mmol), 3-bpp (53.4 mg, 0.384 mmol) and L-ascorbic acid (15 mg, 0.0852 mmol) in 5 ml methanol which had been stirring for 30 min. The combined solutions were then stirred for 5 min then filtered and the solution left to slowly evaporate producing X-ray quality red crystals in 2 days in 23% yield (40 mg). The sample analysed as **2**·3MeOH·$7H_2O$ *viz.* $Fe_4C_{115}H_{137}N_{44}O_{56}Cl_{10}$. Found (calc.%): C 38.00 (38.62), H 3.78 (3.83), N 17.01 (17.23). In the course of the SQUID measurement the sample was heated, cautiously, to 400 K and this then analysed as **2**·H_2O. Found (calc.%): C 39.81 (39.89), H 3.2 (3.35), N 17.93 (18.28).

***cis*-$[Fe_2(NCSe)_4((3,5\text{-}Me_2pz)_3CH)_2(\mu\text{-bpmdc})]{\cdot}2MeCN$ (3)**. 55.9 mg (0.096 mmol) of $[Fe^{II}((3,5\text{-}Me_2pz)_3CH)(OH_2)_3][BF_4]_2$, 27.7 mg (0.192 mmol) of KSeCN, 0.5 ml of an ethanolic solution of bpmdc (21.3 mg, 0.048 mmol) and 15 mg (0.087 mmol) of L-ascorbic acid were dissolved in 10 ml acetonitrile and stirred for 1 h. This solution was then filtered and layered with diethyl ether to produce X-ray quality crystals over a period of 2 weeks, in 60% yield (48 mg). The sample analysed as anhydrous **3**. Found (calc.%): C 46.37 (45.82), H 5.50 (5.13), N 17.27 (17.81).

2.2. Physical measurements

Elemental analyses (CHN) were carried out by Campbell Microanalytical Laboratory, University of Otago, Dunedin, New Zealand. IR spectra were recorded on a Bruker Equinox 55 spectrometer with an ATR sampler provided by Specac Inc., and the samples were run neat.

2.3. X-ray crystallography

X-ray crystallographic measurements were performed at 123(2) K for **1** and **2** and 173(2) K for **3** using a Bruker Smart Apex X8 diffractometer with Mo Kα radiation. Single crystals were mounted on a glass fibre using oil. The data collection and integration were performed within SMART and SAINT+ Software programs, and corrected for absorption using the Bruker SADABS program. Crystallographic data and refinement parameters for **1** and **2** were solved by direct methods (SHELXS-97), and refined (SHELXL-97) by full least-squares on all F^2 data [40]. For **1** all hydrogen atoms were placed in calculated positions. The H-atoms on the solvent water and methanol were omitted but have been included in the crystallographic formula. The asymmetric unit of **1** contains a half of a $[Fe(3\text{-bpp})_2]^{2+}$ monomer, half of the bpmdcK ligand, half of a water molecule, methanol molecule, selenocyanate anion and perchlorate anion. Half a perchlorate anion and half a selenocyanate anion then sit over the same position in the lattice with occupancies

Table 2
Crystallographic data for complexes **1**, **2** and **3**.

	1	**2**	**3**
Formula[a]	$FeC_{48.7}H_{60}N_{15.7}O_{11.2}Se_{1.7}K_1Cl_{1.3}$	$Fe_4C_{115}H_{137}N_{44}O_{56}Cl_{10}$	$Fe_2C_{64}H_{86}N_{22}O_4Se_4$
M_r	1319.79	3609.58	1655.09
Crystal system	Monoclinic	Triclinic	Monoclinic
Space group	*P*2(1)/*m*	*P*-1	*P*2(1)/*c*
a/Å	13.946(1)	11.902(1)	12.275(3)
b/Å	14.415(1)	18.010(1)	18.677(4)
c/Å	14.145(1)	19.001(1)	17.242(3)
α/°	90	85.233(2)	90
β/°	92.225(5)	73.236(2)	103.59(3)
γ/°	90	74.760(2)	90
V/Å^3	2841.4(4)	3762.6(3)	3842.4(13)
T/K	123(2)	123(2)	173(2)
Z	2	1	2
ρ_{calcd}/g cm^{-3}	1.536	1.59	1.431
λ[b]/Å	0.71073	0.71073	0.71073
Ind. reflns	6040	17127	8822
Reflns with $I > 2\sigma(I)$	4233	7954	5713
Parameters	442	1378	440
Restraints	44	91	0
*w R*2[c]	0.2149	0.1845	0.1017
*R*1	0.0977	0.0954	0.0512
Goodness of fit	1.190	1.029	1.026
Largest residuals/e Å^{-3}	2.16, −1.40	0.95, −0.77	1.459, −1.057

[a] Including solvate molecules.
[b] Graphite monochromators.
[c] $R1 = \frac{\sum ||F_o|-|F_c||}{\sum |F_o|}$, $wR2 = \left\{ \frac{\sum [w(F_o^2 \sum F_c^2)^2]}{\sum [w(F_o^2)^2]} \right\}^{1/2}$

based on microanalysis and relative Q peak intensity. One methanol is disordered over two positions while one oxygen (O7) from the perchlorate which sits over the same position as one of the selenocyanate is disordered over two positions. Restraints were placed on the Se–C31 and C31–N11 bond lengths. All non H atoms were refined anisotropically apart from O3, O4, O7, O9, O10, C31 and Cl2 which were restrained using ISOR.

For **2**, all hydrogen atoms were placed in calculated positions, except for the H-atoms on the protonated pyrazolyl nitrogens (H5N, H1N, H6N and H10N), the NH from the bpmdc ligand (H31N) and on the water hydrogen bonded to the bdmpc ligand (H31W, H32W) which were located in the difference maps and allowed to refine freely. The H-atoms on the remaining solvent water molecules were omitted but have been included in the crystallographic formula. The asymmetric unit of **2** contains one complete $[Fe(3\text{-bpp})_2]^{2+}$ monomer and two half occupied $[Fe(3\text{-bpp})_2]^{2+}$ monomers, half of the bpmdc ligand, five perchlorate counter ions, two solvent methanol molecules and eight solvent water molecules. The two half occupied $[Fe(3\text{-bpp})_2]^{2+}$ monomers are refined as completely disordered over two positions, one perchlorate counter ion is disordered over two positions and one methanol molecule and seven water molecules are half occupied. Restraints were placed on the four NH bonds from the pyrazolyls (N1 H1N, N5 H5N, N6 H6N and N10 H10N), on the NH bond from bpmdc (N31 H31N), on the OH bonds from the water hydrogen bonded to the crown ether portion of bdmpc (O3 H31W, O3 H32W) and on four pyridines from the bpp ligand (with nitrogen atoms N13, N18, N23 and N28). All non H atoms were refined anisotropically.

For **3**, all non-hydrogen atoms were refined anisotropically and hydrogens were placed in calculated positions. Data collection parameters, structure solution and refinement details for complexes **1–3** are listed in Table 2. Full details can be found in the CIF files provided in the Supporting information.

2.4. Magnetic measurements

Variable-temperature, solid state direct current (dc) magnetic susceptibility data down to 1.8 K were collected on a Quantum Design MPMS 5T SQUID magnetometer calibrated by use of a standard palladium sample (Quantum Design) of accurately known magnetisation or by use of magnetochemical calibrants such as $CuSO_4{\cdot}5H_2O$. Microcrystalline samples were dispersed in vaseline in order to avoid torquing of the crystallites. The sample mulls were contained in a calibrated gelatine capsule held at the centre of a drinking straw that was fixed at the end of the sample rod.

3. Results and discussion

3.1. Syntheses

Addition of a methanolic solution of $Fe(ClO_4)_2{\cdot}6H_2O$, 3-bpp, KSeCN and L-ascorbic acid to a dichloromethane solution containing 1 ml of an ethanolic solution of bpmdc yields the hydrogen bonded 1D chain $[Fe^{II}(3\text{-bpp})_2][bpmdcK](SeCN)_{1.7}(ClO_4)_{1.3}{\cdot}MeOH{\cdot}H_2O$ (**1**) (*vide infra*). KSeCN is used here as a source of K^+ ions due to its increased solubility in methanol compared to other more commonly used K^+ salts and the K^+ is a guest in the internal crown ether of the bpmdc ligand. This results in the bpmdc ligand adopting the *trans*-pyridyl conformation, with the 4-pyridyl portion of the ligand able to either coordinate to the Fe^{II} ion or act as a hydrogen bond acceptor. Due to both the thermodynamic stability of the $[Fe(3\text{-bpp})_2]^{2+}$ cation and the propensity of the pyrazolyl NH bond to act as a hydrogen bond donor, a hydrogen bonded concertinaed 1D alternating chain of $[Fe^{II}(3\text{-bpp})]^{2+}$ and bpmdcK is formed instead of the 4-pyridyl portion from bpmdcK coordinating directly to the Fe^{II} ion. Di-protonation of the nitrogen atoms of 4,13-diaza-18-crown-6 occurs in the presence of water [41] and similarly subsequent addition of a water/methanol (1:1, v:v) solution of $KClO_4$ and 1 ml of an ethanolic solution of bpmdc to a methanolic solution of $Fe(ClO_4)_2{\cdot}6H_2O$, 3-bpp and ascorbic acid yields $[Fe^{II}(3\text{-bpp})_2]_4[bpmdcH_2(H_2O)_2](ClO_4)_{10}{\cdot}7H_2O{\cdot}3MeOH$ (**2**$\cdot 7H_2O{\cdot}3MeOH$) where the nitrogen atoms from the crown ether portion of bpmdc are protonated and involved in hydrogen bonding to two solvent water molecules sitting above and below the crown. The introduction of water to the reaction scheme has resulted in the

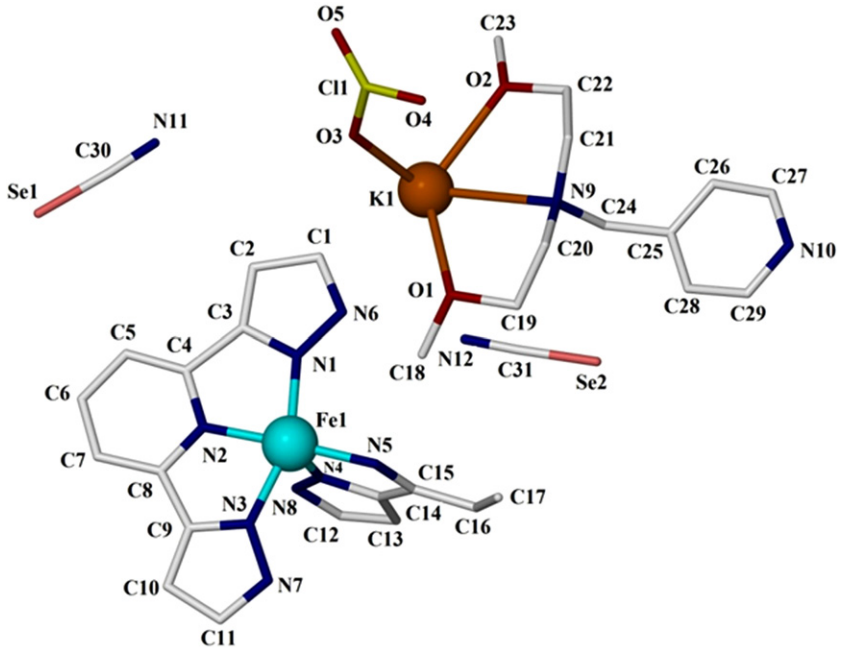

Fig. 1. The asymmetric unit of **1**. Hydrogen atoms removed for clarity.

bpmdc ligand adopting an S-shaped rather than trans-pyridyl conformation as found in **1** conferring a different supramolecular arrangement of the $[Fe^{II}(3\text{-bpp})_2]^{2+}$ monomers in **2** compared to **1** (*vide infra*). Complex **3** was synthesised by reacting the 1:1 precursor $[Fe^{II}((3,5\text{-}Me_2pz)_3CH)(OH_2)_3][BF_4]_2$ [39] with bpmdc and KNCSe in appropriate mole ratios, in ethanol–acetonitrile solution. In comparison to the $[Fe(3\text{-bpp})_2]^{2+}$ products, there was no formation of $[Fe^{II}((3,5\text{-}Me_2pz)_3CH)_2]^{2+}$ which is a little surprising in view of its propensity to form during Fe:ligand 1:1 reactions [36b].

3.2. Description of structures of *1*, *2* and *3*

Complexes **1–3** are shown in Figs. 1–6 and with full details of the bond lengths and angles given in the Supplementary information. Complex **1** crystallises in the monoclinic space group *P*2(1)/m with the Fe(II) ion in a distorted octahedral environment (cis, 79.3(4)–102.5(3)°; trans, 159.0(3)–178.2(4)°; octahedral distortion parameter $\Sigma = 91.76°$) with an average Fe–N bond length measured at 123 K of 1.944 Å, typical of LS Fe^{II}–N values [42]. The Fe(II) ion is surrounded by two meridional 3-bpp ligands forming the monomeric cation $[Fe^{II}(3\text{-bpp})_2]^{2+}$ with two of the non-coordinating NH groups involved in hydrogen bonding to a selenocyanate anion and water molecule (N···N, 2.769 Å and N···O, 2.771 Å, respectively). The remaining two NH groups direct the packing in the structure forming hydrogen bonds to the 4-pyridyl groups of bpmdcK (N···N, 2.755 Å), the K^+ ion present in the internal crown ether site forcing the ligand into the trans-pyridyl configuration with a pyridyl-N to pyridyl-N through space distance of 16.195 Å [17]. Each K^+ ion is in an 8-coordinate hexagonal bipyramidal geometry in the internal crown ether with each K^+ ion bonding to a ClO_4^- anion forming an alternating chain along *b* (K···O, 2.740 Å). The directing NH to 4-pyridyl hydrogen bonds enforce a rigid concertinaed 1D chain of alternating $[Fe^{II}(3\text{-bpp})_2]^{2+}$ cations

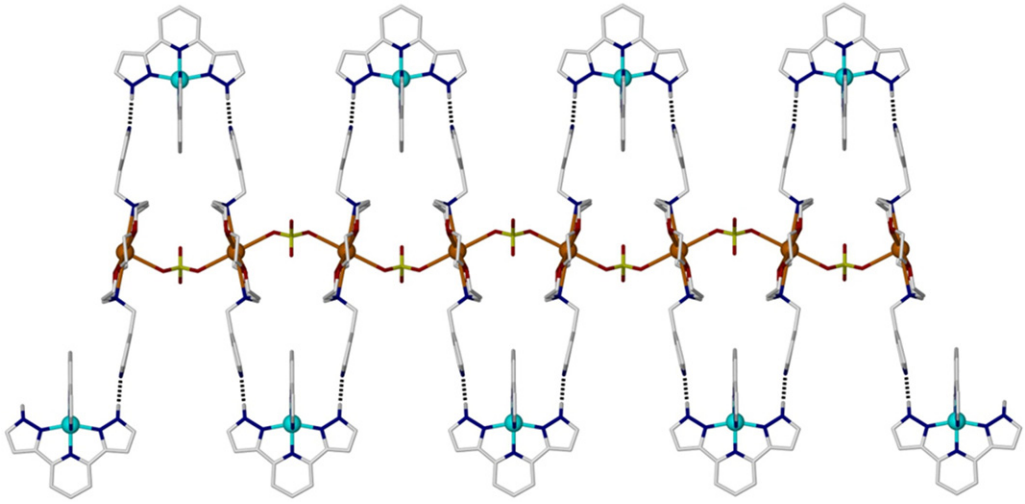

Fig. 2. The packing in **1** with H-bonds shown as dotted lines. The bpmdc 'crown' moieties, with trans pyridyl conformation, are normal to the page. The $NCSe^-$ anions and solvent molecules are not shown, for clarity.

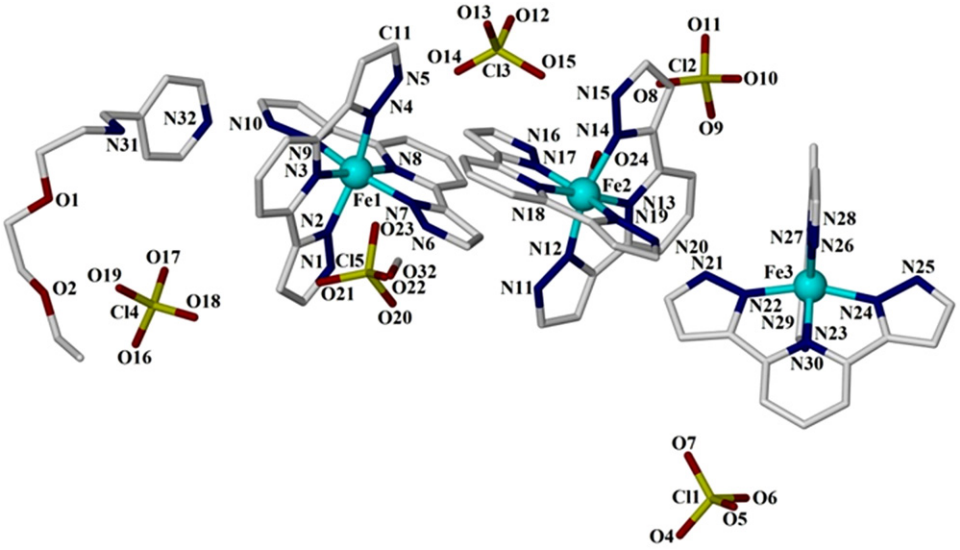

Fig. 3. The asymmetric unit of **2**. Hydrogen atoms removed for clarity.

and bpmdcK ligands lying along the *b* axis. One MeOH solvate and a disordered selenocyanate/perchlorate anion then lie between the hydrogen bonded layers. The water solvate involved in hydrogen bonding to one of the non-coordinating NH groups is involved in two hydrogen bonded pathways. The first involves a hydrogen bond to a perchlorate anion (O···O, 2.900 Å) which subsequently then coordinates through the K^+ ion in the crown. This pathway is then symmetry generated through to a $[Fe(3\text{-bpp})_2]^{2+}$ cation on a neighbouring 1D chain. The second pathway involves hydrogen bonds to the nitrogen on a partially occupied NCSe anion (O···N, 2.763 Å) and to a partially occupied perchlorate anion (O···O, 3.151 Å). The disordered oxygen (O7) on the partially occupied perchlorate anion is then hydrogen bonded to the disordered oxygen on the methanol (O···O, 2.571 Å).

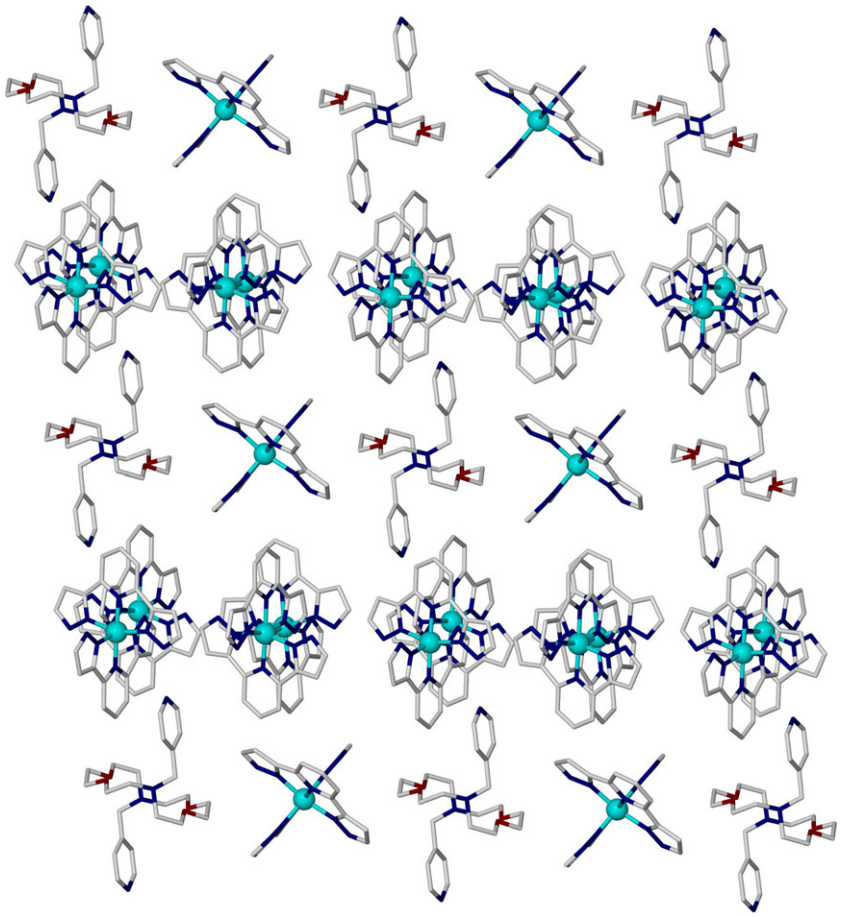

Fig. 4. Packing of **2**. Hydrogen atoms, anions, solvate oxygens and methanols removed for clarity.

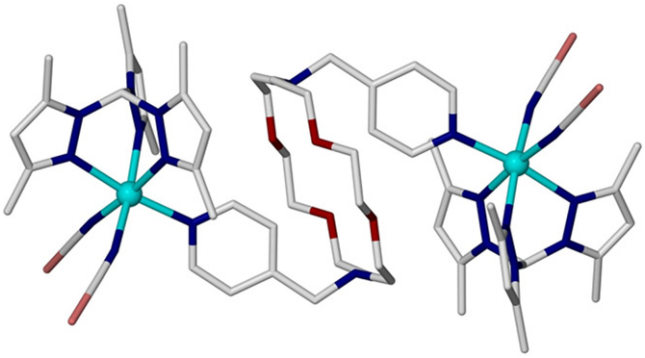

Fig. 5. The molecular structure of **3**. Hydrogen atoms and solvent omitted for clarity. Oxygen – red; nitrogen – dark blue; iron(II) turquoise. The MeCN solvate molecules are omitted for clarity.

Complex **2** crystallises in the triclinic space group *P*-1 with one complete $[Fe^{II}(3\text{-bpp})_2]^{2+}$ and two half occupied $[Fe^{II}(3\text{-bpp})_2]^{2+}$ monomers in the ASU (Fig. 3). Each Fe(II) ion is in a distorted octahedral geometry (cis, 79.1(3)–102.9(2)°, 77.0(7)–103.2(8)°, 78.1(7)–103.2(7)°; trans, 158.8(2)–178.1(3)°, 157.4(5)–176.1(12)°, 157.1(4)–177.2(12)°; octahedral distortion parameter [42] Σ = 93.9°, 92.42°, 92.35° for Fe1, Fe2 and Fe3, respectively) with an average Fe–N bond length measured at 123 K of 1.947 Å for Fe1, 1.937 Å for Fe2 and 1.947 Å for Fe3, typical for LS Fe^{II}–N values. Each Fe(II) ion is surrounded by two meridional 3-bpp ligands forming the $[Fe^{II}(3\text{-bpp})_2]^{2+}$ cations. The cations associated with Fe1 and Fe2 form a layer of terpy like embraces which alternates between a diagonal row of single Fe2 cations and a diagonal row of pairs of the Fe1 cations. One of the four non-coordinating pyrazole NH groups in the Fe1 cation is then involved in hydrogen bonding to the 4-pyridyl group of the bpmdc ligand which then forms hydrogen bonds to the Fe1 cation of another layer (N···N, 2.750 Å) via its second 4-pyridyl group. The Fe3 cation then lies between the layers of Fe1 and Fe2 cations and between these bpmdc ligands (Fig. 4). The remaining three non-coordinating pyrazole NH groups from the Fe1 cation then form hydrogen bonds to one fully occupied perchlorate anion (N···O, 2,850 Å), one disordered perchorate anion (N···O14, 2.884 Å, N···O14′, 2.972 Å) and one methanol molecule (N···O, 2.742 Å). The four non-coordinating pyrazole NH groups of the Fe2 cation form hydrogen bonds to three water molecules (N···O, 2.710, 2.753, 2.810 Å) and one methanol molecule (N···O, 2.740 Å). The four non-coordinating pyrazole NH groups from the Fe3 cation then form hydrogen bonds to four water molecules (N···O, 2.720, 2.716, 2.775, 2.692 Å). In terms of intermolecular interactions the first one to consider is the edge-to-face (ef) and offset face-to-face (off) interactions found in the layer of Fe1 and Fe2 cations. The off interactions between Fe1 cations have pyrazole centroid to centroid distances of 3.923 and 4.022 Å and ef interactions with C – centroid distances of 3.467 and 3.737 Å. The Fe2 cations are completely disordered over two positions with off interactions having pyrazole centroid to centroid distances of 3.624, 3.635, 3.988 and 4.226 Å and ef interactions having distances of 3.599, 3.666, 3.723 and 3.992 Å. The Fe1 cation has a hydrogen bond pathway via a perchlorate anion (N···O, 2.850 Å), a water molecule (O···O, 2.815 Å) leading to the Fe2 cation (O···O, 2.710 Å). A second pathway from the Fe1 cation proceeds via the disordered perchlorate anion (N···O, 2.847, 3.111 Å) and a water molecule (O···O, 2.587, 3.125 Å) leading to the NH group on the Fe3 cation (O···N, 2.716 Å). The bpmdc ligand has a pyridyl N-N distance of 13.328 Å and is in a gentle S-shaped conformation in **2** (Fig. 6), in direct contrast to the 1D complex $[Co(NCS)_2(H_2O)_2(bpmdc)]$ found in Ref. [17] which had a pyridyl N-N distance of 16.566 Å and was in the trans-pyridyl conformation, the pyridyl N atoms being covalently bonded to Co^{II}. Both complex **2** and the abovementioned Co^{II} complex [17] have two waters hydrogen bonded above and below the crown with the difference in the conformation of the bpmdc ligand presumably due to the hydrogen bonding between the pyrazole

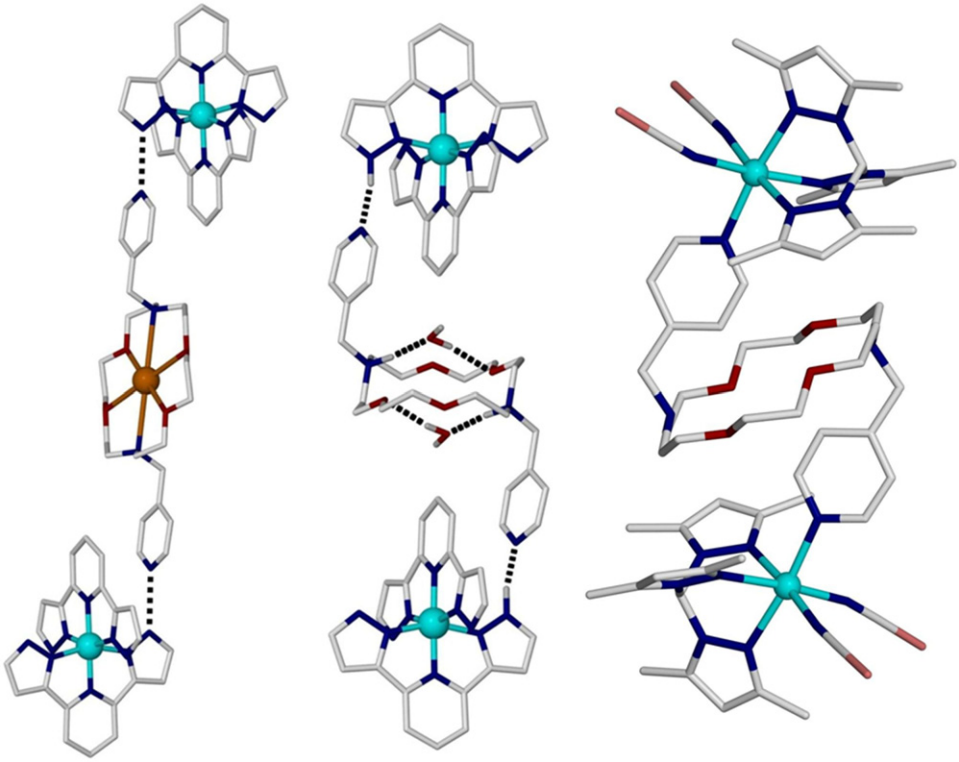

Fig. 6. Comparison of the supramolecular packing involving the crown ligand, bpmdc, in **1**–**3**.

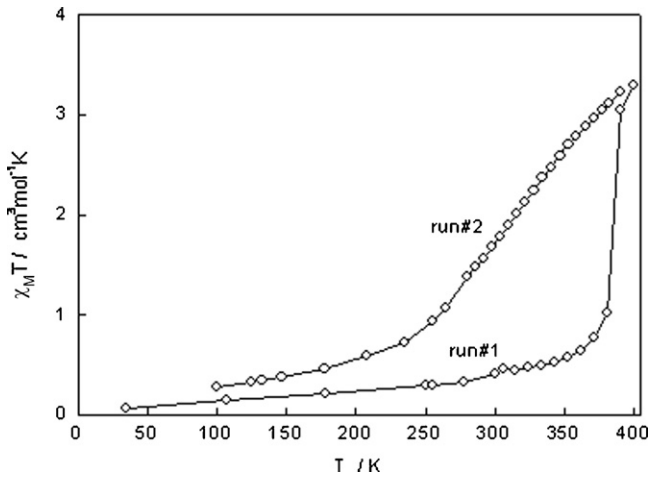

Fig. 7. Plot of $\chi_M T$ vs. temperature for complex **1**. Run #1 heating from 35 K to 400 K, run #2 cooling from 400 K to 100 K.

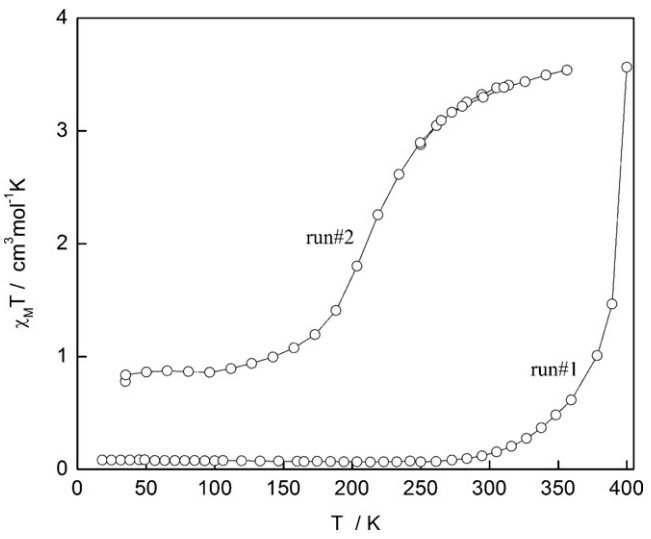

Fig. 8. Plot of $\chi_M T$ vs. temperature for complex **2**. Run #1 heating from 18 K to 400 K, run #2 cooling 356 K to 35 K.

NH group and the pyridyl group on bpmdc forcing a certain packing arrangement.

Complex **3** crystallises in the monoclinic space group $P2_1/c$ with the symmetrically equivalent Fe(II) ions in a distorted octahedral geometry (cis, 81.9(1)–94.3(1)°; trans, 171.7(1)–175.1(1)°; octahedral distortion parameter Σ = 43.5° [42]; compared to 46.0° in the μ-4,4′-bipy analogue [36c]) with an average Fe–N bond length measured at 173 K of 2.178 Å, typical of HS Fe^{II} ions. Each Fe(II) ion is capped by one facial tridentate $(3,5\text{-}Me_2pz)_3CH$ ligand and with two *cis* selenocyanate anions occupying a further two coordinate sites. As seen in Figs. 5 and 6, the bpmdc ligand adopts the compact S-shaped conformation with a pyridyl-N to pyridyl-N through space distance of 8.190 Å, similar to that found in the 1D complex $[Co(bpmdc)Cl_2]\cdot MeOH$ [17], and bridges via the remaining coordination site on each $\{[Fe(NCSe)_2((3,5\text{-}Me_2pz)_3CH)\}$ moiety forming the dinuclear complex *cis*-$[Fe_2(NCSe)_4((3,5\text{-}Me_2pz)_3CH)_2(\mu\text{-bpmdc})]\cdot 2MeCN$ (**3**). Two acetonitrile solvent molecules then sit in the void between neighbouring dimers with no directing intermolecular interactions present in the crystal lattice.

3.3. Magnetic studies

Direct current (dc) magnetic susceptibility studies were performed on microcrystalline samples of **1** and **2** in the 10–400 K range under an applied field of 5 kG and are shown in Figs. 7 and 8. The $\chi_M T$ values shown are per Fe(II). Upon heating, complex **1** shows an abrupt SCO transition with a $T_{1/2}$ of ~384 K The $\chi_M T$ value increases gradually from 0.0695 cm^3 mol^{-1} K at ~35 K, typical of LS (low spin) Fe(II), to 0.405 cm^3 mol^{-1} K at ~300 K, where upon it increases rapidly up to a value of 3.296 cm^3 mol^{-1} K at ~400 K, typical of HS (high spin) Fe(II). However upon cooling this SCO transition is not reversible and a gradual SCO transition with $T_{1/2}$ of ~303 K can be seen where the $\chi_M T$ value gradually decreases from the value of 3.296 cm^3 mol^{-1} K reached upon heating up to ~400 K down to 0.729 cm^3 mol^{-1} K at ~235 K, where upon it decreases at a more gradual rate down to 0.282 cm^3 mol^{-1} K at ~100 K. This behaviour can be attributed to loss of one water and one methanol upon heating to 400 K.

The $\chi_M T$ vs. temperature plots upon heating are similar for complex **1** and **2** with complex **2** showing an abrupt SCO transition with a $T_{1/2}$ of 392 K. The $\chi_M T$ increases gradually from 0.0832 cm^3 mol^{-1} K at ~18 K, typical of LS Fe(II), to 0.155 cm^3 mol^{-1} K at ~305 K, where upon it increases rapidly up to a value of 3.564 cm^3 mol^{-1} K at ~400 K, typical of HS (high spin) Fe(II). Again upon cooling this SCO transition is not reversible and a gradual incomplete SCO transition with $T_{1/2}$ of ~216 K emerges where the $\chi_M T$ value gradually decreases from the value of 3.564 cm^3 mol^{-1} K reached upon heating up to ~400 K down to 0.939 cm^3 mol^{-1} K at ~127 K where it then plateaus eventually reaching a $\chi_M T$ value of 0.779 cm^3 mol^{-1} K. This incomplete SCO transition is fully reversible and can be attributed to the loss of 5 water molecules and 3 methanol molecules when heated to 400 K.

The loss of solvent upon heating changes the $T_{1/2}$ values from 384 K to 303 K for **1** and from 392 K to 216 K for **2**, with a change from an abrupt transition at a higher $T_{1/2}$ to a gradual SCO transition at a lower $T_{1/2}$ present in complexes **1** and **2**. In the $[Fe(3\text{-bpp})_2]X_2\cdot H_2O$ series of salts (see Table 1 and the review in Ref. [12], Section 3.1.2) the $T_{1/2}$ values generally decrease and the SCO transition changes from gradual to abrupt in character as one proceeds from the hydrated to the anhydrous form. The higher $T_{1/2}$ in the solvated samples **1** and **2** as compared to the partially solvated samples probably derives from the hydrogen bonding between the pyrazole NH group and lattice methanol, water, bpmdc ligand and associated anions. This weakens the N–H bond, increasing the electron density of the coordinating imine nitrogen, strengthening the nitrogen–iron bond and therefore stabilising the LS Fe(II) state. Upon heating, complexes **1** and **2** lose some of their lattice solvent with a subsequent stabilisation of the HS Fe(II) state pushing the $T_{1/2}$ value to lower temperatures. In complexes **1** and **2** we see the decrease in $T_{1/2}$ occurring as in the $[Fe(3\text{-bpp})_2]X_2\cdot H_2O$ series, however as we proceed from the fully solvated to the partially solvated form the SCO transition changes from abrupt to gradual which is in direct contrast to $[Fe(3\text{-bpp})_2]X_2\cdot H_2O$. In $[Fe^{II}(3\text{-bpp})_2][BF_4]_2\cdot 3H_2O$ the NH groups from each pyrazolyl moiety are involved in a hydrogen bonding network containing water molecules and tetrafluoroborate ions [13] and it has been suggested that the anhydrous $[Fe^{II}(3\text{-bpp})_2][BF_4]_2$ adopts a form of crystal packing allowing offset face-to-face and edge-to-face aryl–aryl interactions and it is this that is the origin of the cooperativity leading to the abrupt and hysteretic SCO transition [14]. It is not possible for **1** to adopt such a conformation because of the stronger hydrogen bonded network formed by the bpmdc ligand and, as a consequence, we suggest this is why we see a gradual SCO transition, with $T_{1/2}$ of 303 K.

Complex **2** has a layer of $[Fe^{II}(3\text{-bpp})]_2^{2+}$ cations exhibiting the aforementioned aryl–aryl interactions linked by hydrogen bonded bpmdc ligands but is prevented from reaching the full complement

of aryl–aryl interactions by the bpmdc ligand resulting in an almost complete SCO transition, with $T_{1/2}$ of 216 K. This $T_{1/2}$ value is more in keeping with the values associated with the anhydrous salts $[Fe(3\text{-bpp})_2]X_2$, and is reasonable given that **2** could be viewed as a partially disrupted form of the crystal packing described above for anhydrous $[Fe^{II}(3\text{-bpp})_2][BF_4]_2$. This suggests the cooperativity between the Fe(II) ions leading to the abrupt SCO transition is largely solvent dependent and not through the hydrogen bonded bpmdc ligand which is reasonable given the size and nature of the ligand and the expectation that it would not be conducive to any strong cooperative effects.

The $\chi_M T$ vs. temperature data for the dinuclear complex **3** shows a constant value between 300 and ~50 K, of 3.4 $cm^3\ mol^{-1}$ K (per Fe), indicative of high-spin Fe(II) centres with no intradinuclear exchange coupling. Below 50 K, a rapid decrease in $\chi_M T$ is observed due to zero-field splitting effects (Supp. Info. Fig. SI 3). Thus, in **3** and the μ-4,4′-bipy analogue [36c], the structural and magnetic data are indicative of no spin-crossover occurring.

4. Conclusions

Three new Fe^{II} compounds containing the di-pyridyl functionalised diaza-18-crown-6 ligand, bpmdc, have been structurally characterised, two (**1** and **2**) displaying supramolecular arrays involving the spin crossover $[Fe(3\text{-bpp})_2]^{2+}$ cations. Changing the guest in, or near, the crown ether portion of the bpmdc ligand has afforded different supramolecular packing arrangements of the $[Fe(3\text{-bpp})_2]^{2+}$ cation leading to an abrupt SCO transition at a higher $T_{1/2}$ than that of more conventional $[Fe(3\text{-bpp})_2](anion)_2$ salts. Subsequent heating of complexes **1** and **2** causes the loss of solvent from the lattice leading to a change in the $T_{1/2}$ of both samples. The pyridyl arms of the bpmdc ligand, despite their usual propensity for coordinating to Fe^{II}, act as hydrogen-bond donors in **1** and **2**, thus offering a route to the packing of simple monomeric SCO salts while barely affecting the ligand field around the metal. Changing the 'end tridentate caps', from the meridional 3-bpp, to the facial $(3,5\text{-}Me_2pz)_3CH$, led to isolation of the covalently bridged complex **3**, in which the Fe(II) centres remain high-spin at all temperatures as judged by crystallography and magnetism.

Finally, we note that metallo-supramolecular and multifunctional aspects of spin crossover compounds have been recently reviewed [43].

Supplementary data

Tables of bond distances and angles for **1**–**3** are provided; Tables SI 1–6. Two figures of packing diagrams for **1**; Figs. SI 1 and SI 2. Magnetism for *cis*-$[Fe^{II}_2(NCSe)_4((3,5\text{-}Me_2pz)_3CH)_2(\mu\text{-bpmdc})]\cdot 2MeCN$ (**3**); Fig. SI 3. Other crystallographic details are in the CIFs. Full crystallographic data for **1**–**3** are available on request from the Cambridge Crystallographic Data Centre, 12 Union Road, CambridgeCB2 1EZ, UK (http://www.ccdc.cam.ac.uk/). CCDC numbers 802609 (**1**), 802610 (**2**), 802611 (**3**).

Acknowledgements

We thank Dr Martin Duriska for assistance with synthesis of the crown ligand, bpmdc. The work was supported financially by Australian Research Council Discovery grants to SRB and KSM.

Appendix A. Supplementary data

Supplementary data associated with this article can be found, in the online version, at doi:10.1016/j.ccr.2011.01.033.

References

[1] See articles in: P. Gütlich, H.A. Goodwin (Eds.), Spin-crossover in Transition-metal Compounds, Top. Curr. Chem., vol. 233–235, Springer, Berlin, 2004.
[2] P. Gütlich, A. Hauser, H. Spiering, Angew. Chem. Int. Ed. 33 (1994) 2024.
[3] O. Kahn, J. Kröber, C.J. Martinez, Adv. Mater. 4 (1992) 718.
[4] (a) P. Gütlich, Y. Garcia, H.A. Goodwin, Chem. Soc. Rev. 29 (2000) 419;
(b) O. Kahn, Nature 21 (1999) 319.
[5] (a) K.S. Murray, C.J. Kepert, Top. Curr. Chem. 233 (2004) 195;
(b) Y. Garcia, V. Niel, M.C. Muñoz, J.A. Real, Top. Curr. Chem. 233 (2004) 229;
(c) J.A. Real, A.B. Gaspar, V. Niel, M.C. Muñoz, Coord. Chem. Rev. 236 (2003) 121.
[6] (a) S. Arata, H. Torigoe, T. Iihoshi, N. Matsumoto, F. Dahan, J.-P. Tuchagues, Inorg. Chem. 44 (2005) 9288;
(b) D.L. Reger, J.R. Gardinier, W.R. Gemmil, M.D. Smith, A.M. Shahin, G.J. Long, L. Rebbouh, F. Grandjean, J. Am. Chem. Soc. 127 (2005) 2303.
[7] S. Hayami, Y. Shigeyoshi, M. Akita, K. Inoue, K. Kato, K. Osaka, M. Takata, R. Kawajiri, T. Mitani, Y. Maeda, Angew. Chem. Int. Ed. 44 (2005) 4899.
[8] (a) M. Yamada, M. Ooidemizu, Y. Ikuta, S. Osa, N. Matsumoto, S. Iijima, M. Kojima, F. Dahan, J.-P. Tuchagues, Inorg. Chem. 42 (2003) 8406;
(b) G.S. Matouzenko, G. Molnar, N. Brefuel, M. Perrin, A. Bousseksou, S.A. Borshch, Chem. Mater. 15 (2003) 550;
(c) Y. Ikuta, M. Ooidemizu, Y. Yamahata, M. Yamada, S. Osa, N. Matsumoto, S. Iijima, Y. Sunatsuki, M. Kojima, F. Dahan, J.-P. Tuchagues, Inorg. Chem. 42 (2003) 7001;
(d) Y. Sunatsuki, Y. Ikuta, N. Matsumoto, H. Ohta, M. Kojima, S. Iijima, S. Hayami, Y. Maeda, S. Kaizaki, F. Dahan, J.-P. Tuchagues, Angew. Chem. Int. Ed. 42 (2003) 1614.
[9] (a) J.F. Létard, P. Guionneau, E. Codjovi, O. Lavastre, G. Bravic, D. Chasseau, O. Kahn, J. Am. Chem. Soc. 119 (1997) 10861;
(b) S. Hayami, Z.-Z. Gu, M. Shiro, Y. Einaga, A. Fujishima, O. Sato, J. Am. Chem. Soc. 122 (2000) 7126;
(c) R. Boča, M. Boča, L. Dlháň, M. Vrbová, R. Werner, Inorg. Chem. 40 (2001) 3025;
(d) J.A. Real, B. Gallois, T. Granier, F. Suez-Panamá, J. Zarembowitch, Inorg. Chem. 31 (1992) 4972;
(e) Z.-J. Zhong, J.-Q. Tao, Z. Yu, C.-Y. Duan, Y.-J. Liu, X.-Z. You, J. Chem. Soc., Dalton Trans. (1998) 327.
[10] O. Kahn, C.J. Martinez, Science 279 (1998) 44.
[11] (a) M. Halcrow, Coord. Chem. Rev. 249 (2005) 2880;
(b) M. Halcrow, Coord. Chem. Rev. 253 (2009) 2493.
[12] J. Olguin, S. Brooker, Coord. Chem. Rev. 255 (2011) 203.
[13] (a) K.H. Sugiyarto, H.A. Goodwin, Aust. J. Chem. 41 (1988) 1645;
(b) K.H. Sugiyarto, D.C. Craig, D. Rae, H.A. Goodwin, Aust. J. Chem. 47 (1994) 869.
[14] K.H. Sugiyarto, W.-A. McHale, D.C. Craig, A.D. Rae, M.L. Scudder, H.A. Goodwin, Dalton Trans. (2003) 2443.
[15] H.A. Goodwin, K.H. Sugiyarto, Chem. Phys. Lett. 139 (1987) 470.
[16] T. Buchen, P. Gütlich, H.A. Goodwin, Inorg. Chem. 33 (1994) 4573.
[17] M.B. Duriska, S.M. Neville, S.R. Batten, Chem. Commun. (2009) 5575.
[18] K.H. Sugiyarto, K. Weitzner, D.C. Craig, H.A. Goodwin, Aust. J. Chem. 50 (1997) 869.
[19] T. Buchen, P. Gütlich, K.H. Sugiyarto, H.A. Goodwin, Chem. Eur. J. 2 (1996) 1134.
[20] K.H. Sugiyarto, M.L. Scudder, D.C. Craig, H.A. Goodwin, Aust. J. Chem. (2000) 755.
[21] A. Bhattacharjee, V. Ksenofontov, K.H. Sugiyarto, H.A. Goodwin, P. Gütlich, Adv. Funct. Mater. 13 (2003) 877.
[22] (a) Y. Maeda, M. Suzuki, S. Hirose, S. Hayami, T. Oniki, S. Sugihara, Bull. Chem. Soc. Jpn. 71 (1998) 2837;
(b) R. Hernández-Molina, A. Mederos, S. Dominguez, P. Gili, C. Ruiz-Pérez, A. Castineiras, X. Solans, F. Lloret, J.A. Real, Inorg. Chem. 37 (1998) 5102.
[23] E. Coronado, M.C. Gimènez-Lopez, C. Gimenez-Saiz, J.M. Martinez-Agudo, F.M. Romero, Polyhedron 22 (2003) 2375.
[24] S. Marcén, L. Lecren, L. Capes, H.A. Goodwin, J.-F. Lètard, Chem. Phys. Lett. 358 (2002) 87.
[25] M.L. Scudder, D.C. Craig, H.A. Goodwin, Crystengcomm 7 (2005) 642.
[26] E. Coronado, J.R.G. Mascarós, M.C. Giménez-López, M. Almeida, J.C. Waerenborgh, Polyhedron 26 (2007) 1838.
[27] M. Clemente-León, E. Coronado, M. Carmen Giménez-López, F.M. Romero, Inorg. Chem. 46 (2007) 11266.
[28] M.C. Giménez-López, M. Clemente-León, E. Coronado, F.M. Romero, S. Shova, J. Tuchagues, Eur. J. Inorg. Chem. (2005) 2783.
[29] D. Fedaoui, Y. Bouhadja, A. Kaiba, P. Guionneau, J.-F Létard, P. Rosa, Eur. J. Inorg. Chem. (2008) 1022.
[30] E. Coronado, J.C. Dias, M.C. Giménez-López, C. Giménez-Saiz, C.J. Gómez-Garcia, J. Mol. Struct. 890 (2008) 215.
[31] D.A. Bardwell, J.C. Jeffrey, P.L. Jones, J.A. McCleverty, E. Psillakis, Z. Reeves, M.D. Ward, J. Chem. Soc., Dalton Trans. (1997) 2079.
[32] G. Dong, J.P. Matthews, D.C. Craig, A.T. Baker, Inorg. Chim. Acta 284 (1999) 266.
[33] T.M. Ross, S.R. Batten, B. Moubaraki, K.S. Murray, in preparation.
[34] D.L. Reger, C.A. Little, M.D. Smith, A. Rheingold, K. Lam, T. Concolino, G.J. Long, R. Hermann, F. Grandjean, Eur. J. Inorg. Chem. (2002) 1190.
[35] B. Moubaraki, B.A. Leita, G. Halder, S.R. Batten, P. Jensen, J. Smith, J.D. Cashion, C. Kepert, J.F. Létard, K.S. Murray, Dalton Trans. (2007) 4413.
[36] (a) C.J. Schneider, B. Moubaraki, J.D. Cashion, D.R. Turner, B.A. Leita, S.R. Batten, K.S. Murray, submitted for publication;
(b) S.R. Batten, J. Bjernemose, P. Jensen, B.A. Leita, K.S. Murray, B. Moubaraki,

J.P. Smith, H. Toftlund, Dalton Trans. (2004) 3370;
(c) A.A. Salaudeen, C.A. Kilner, M.A. Halcrow, Polyhedron 27 (2008) 2569.
[37] (a) B. Dietrich, J.-M. Lehn, J.P. Sauvage, J. Blanzat, Tetrahedron 29 (1973) 1629;
(b) H. Tsukube, K. Yamashita, T. Iwachido, M. Zenki, J. Org. Chem. 56 (1991) 268.
[38] P. Gamez, R.H. Steensma, W.L. Driessen, J. Reedijk, Inorg. Chim. Acta 333 (2002) 51.
[39] D.L. Reger, C.A. Little, A.L. Rheingold, R. Sommer, G.J. Long, Inorg. Chim. Acta 316 (2001) 65.
[40] (a) G.M. Sheldrick, SHELXL-97, Program for Refinement of Crystal Structures, University of Göttingen, Germany, 1997;
(b) A.L. Spek, Acta. Crystallogr. Sect. A 46 (1990) C34.
[41] S.J. Dalgarno, C.L. Raston, Dalton Trans. (2003) 287.
[42] P. Guionneau, M. Marchivie, G. Bravic, J.-F. Létard, D. Chasseau, Top. Curr. Chem. 234 (2004) 97.
[43] Y. Bodenthin, G. Schwarz, Z. Tomkowicz, M. Lommel, Th. Geuef, W. Haase, H. Möhwald, U. Pietsch, D.G. Kurth, Coord. Chem. Rev. 253 (2009) 2414.